Ao Zhou, Shaohua Ju*, Sivasankar Koppala, Lei Xu, Jinhui Peng and Shihong Tian

Extraction of In^{3+} and Fe^{3+} from sulfate solutions by using a 3D-printed "Y"-shaped microreactor

https://doi.org/10.1515/gps-2018-0045
Received March 7, 2018; accepted July 20, 2018; previously published online September 3, 2018

Abstract: In traditional large-scale industrial applications of solvent extraction, there are some limitations such as low extraction efficiency, emulsification, co-extraction, and potential safety hazards. Recently, the application of microfluidic technology in solvent extraction has been dedicated to avoid the above problems effectively. However, manufacturing microchannels becomes a key problem before the application of such a new technology. In this article, the design and fabrication of a "Y"-shaped microreactor by using a three-dimensional (3D) printer, and its feasibility for extraction and separation, is illustrated. The extraction performance of a "Y"-shaped microreactor was investigated by carrying out the extraction of In^{3+} and Fe^{3+} from a sulfate solution under different experimental conditions. When the residence time was 210 s, the volume fraction of extractant (D2EHPA) was 30%, and the initial pH value of the aqueous solution was 0.7, the extraction rate of In^{3+} and the separation coefficient $\beta_{In/Fe}$ were 98.07% and 1593, respectively. Remarkably, the handling capacity of the 3D-printed "Y" microreactor presented in this work with a channel length of 36 mm was superior, whereas the extraction rate of In^{3+} was very close to that of the previously reported microchip with a channel length of 120 mm.

Keywords: 3D printing; indium; microreactor; separation; solvent extraction.

1 Introduction

Indium is a kind of scattered metal widely used in high-technology fields such as computer, national defense, military, nuclear industry, and modern information industries. The general principle of indium extraction is as follows: indium-containing material→enrichment→leaching→extraction or purification→replacement→sponge indium→electrolytic refining→indium [1]. Indium minerals are often found in sulfides of nonferrous metals. Because of their low grade, indium cannot be directly extracted from minerals. A typical material for extracting indium is a zinc oxide dust, a by-product from zinc hydrometallurgy [2]. When indium is extracted from the dust, an extraction or purification process is usually carried out before the reduction process [3].

In industrial production, mixing-settler equipment is commonly used in the solvent extraction process, which has disadvantages such as emulsification, co-extraction, large amount of extractant consumption, and others [4, 5]. To obtain adequate extraction rate and separation effect, longer reaction duration, multistage extraction, and separation stripping process are required, thereby increasing the complexity of the extraction process. In contrast, the rapid development of microfluidic technology in recent years solves the above problems. In the extraction process based on microfluidic technology, due to the reduction of channel size inside the microreactor to micron level, the gradient of some physical parameters such as temperature, concentration, pressure, and density increases dramatically [6]. This enhances the heat transfer and mass transfer driving forces, thereby increasing the diffusion flux and decreasing the mixing time [7, 8]. Many studies have confirmed that microfluidic extraction technology has a very excellent extraction performance [9]. Li et al. [10] reported

***Corresponding author: Shaohua Ju,** Faculty of Metallurgical and Energy Engineering, Kunming University of Science and Technology, Kunming 650093, Yunnan, China; Key Laboratory of Unconventional Metallurgy, Kunming University of Science and Technology, Kunming 650093, Yunnan, China; State Key Laboratory of Complex Nonferrous Metal Resources Clean Utilization, Kunming 650093, Yunnan, China; and Key Laboratory of Intensification Metallurgy, Kunming University of Science and Technology, Kunming 650093, Yunnan, China, e-mail: shj_200801@126.com
Ao Zhou, Sivasankar Koppala and Shihong Tian: Faculty of Metallurgical and Energy Engineering, Kunming University of Science and Technology, Kunming 650093, Yunnan, China; Key Laboratory of Unconventional Metallurgy, Kunming University of Science and Technology, Kunming 650093, Yunnan, China; and State Key Laboratory of Complex Nonferrous Metal Resources Clean Utilization, Kunming 650093, Yunnan, China
Lei Xu and Jinhui Peng: Faculty of Metallurgical and Energy Engineering, Kunming University of Science and Technology, Kunming 650093, Yunnan, China; Key Laboratory of Unconventional Metallurgy, Kunming University of Science and Technology, Kunming 650093, Yunnan, China; State Key Laboratory of Complex Nonferrous Metal Resources Clean Utilization, Kunming 650093, Yunnan, China; and Key Laboratory of Intensification Metallurgy, Kunming University of Science and Technology, Kunming 650093, Yunnan, China

that the extraction rate of In^{3+} increased from 81.2% to 99.9% when the contact reaction time ranged from 0.3 to 0.5 s, and the maximum cross-sectional area volume ratio reached approximately 12,000 m^2/m^3, in the double "Y" type microchannel with a feature size of approximately 100 μm. However, the handling capacity of extraction in the microreactor is very low, approximately 0.02 μl/min. Although a high rate of single stage extraction could be achieved, it is difficult to expand the existing conventional methods for use in actual production [11].

Furthermore, fabricating microreactors using traditional processing methods has the following limitations: huge and complex equipment, low utilization rate of raw materials, relatively long production cycles, and high costs [12, 13]. These shortcomings can be dealt with using an emerging technology – three-dimensional (3D) printing – in which digital documents can be converted into dimensional solids by using 3D printing technology. The 3D printing technology is a method of producing a material layer by layer, it will not increase the processing cost even if the reactor is with a very complex structure, and thus the rapid manufacture of microreactor with complex structure can be realized [14, 15]. In addition, it is convenient to improve and optimize the microreactor design, which can effectively shorten the design cycle. Therefore, making good use of 3D printing technology can be a low-cost and highly efficient process to transform a single channel microreactor into a multichannel microreactor [16]. Additionally, it can solve the problems of reaction enlargement, excessive consumption of extractant, co-extraction in industrial extraction equipment, together with the advantages of high specific surface area and high mass transfer efficiency of the microreactor [17, 18].

Three-dimensional printing, commonly referred to as additive manufacturing technologies or rapid prototyping technologies, has widely spread in many different fields including physical prototypes, tissue engineering, electronics devices, microfluidics, and high specific strength materials. Compared with conventional manufacturing technologies, 3D printing technology shows its unique advantages such as freedom of design and tool-less fabrication [19]. In many fields of 3D printing technology, fused deposition modeling (FDM) and ultraviolet-assisted 3D printing (UV-3D) are considered to be relatively common forms of printing method. The FDM requires mechanical and thermal properties of the printing materials, so thermoplastic polymer filaments (ABS, PLA, and a few others) are used as structural inks. Also, due to the limitation of material properties and extrusion processing methods, the printing accuracy of FDM is affected [20].

In contrast, UV-3D is better at printing accuracy. The printing raw material of this technology is constituted by a photo cross-linkable resin system, which can be accurately treated using UV light irradiation at room temperature [21]. In this area, many works have focused on the realization of functional 3D structures, which partially overcome the fundamentally limited mechanical properties of resin systems. For example, Invernizzi et al. [21] studied the development of new dual-cure interpenetrating polymer networks (IPN) based on photocurable acrylics and thermocurable anhydride epoxy systems, and found that by incorporating reinforcing fibers into the novel dual-cure polymeric matrix, carbon fiber-reinforced and glass-fiber-reinforced composite formulations could be obtained. Chen et al. [22] investigated a UV-assisted 3D printing of thermally cured epoxy composites with high tensile toughness via a two-stage curing approach. They found that the printed IPN epoxy composites enabled by the two-stage curing show isotropic mechanical properties and high tensile toughness. Credi et al. [23] studied the fabrication of monolithic Unibody lab-on-a-chip integrating bioactive micrometric 3D scaffolds by multimaterial stereolithography. They successfully synthesized a novel biotin-conjugated photopolymer, which was demonstrated by the stereo-lithography fabrication of biotinylated structures smaller than 100 μm.

Based on the above considerations, in this article, we demonstrate the extraction of In^{3+} and Fe^{3+} by using UV-3D-printed "Y" microreactor. The effects of initial pH value of aqueous phase, residence time, and phase ratio (O/A) on the extraction of In^{3+} and Fe^{3+} were investigated and compared with the experimental results of conventional oscillating extraction method. The results indicated that the liquid–liquid extraction and separation technology by using a 3D-printed microreactor is feasible. It has also laid the data foundation for the experiments of 3D printing multichannel microreactor to amplify the handling capacity of solvent extraction and separation [24].

2 Materials and methods

2.1 Materials and analysis

The analytical pure extractant D2EHPA ($C_{16}H_{35}O_4P$) and the solvent (260# solvent oil) used for diluting the extractant were purchased from Luoyang AODA Chemical Co. Ltd. (Luoyang, China). The organic phase was prepared by mixing a certain amount of D2EHPA in 260# solvent oil. The aqueous phase was prepared by dissolving analytically pure $In_2(SO_4)_3 \cdot 9H_2O$ and $Fe_2(SO_4)_3$, purchased from Ruijin

Tianjin Special Chemicals Co. Ltd. (Tianjin, China), in deionized water produced by using the laboratory water purification system Eco-Q30, Shanghai Hetai Instrument Co. Ltd. (Shanghai, China) The aqueous phase was adjusted to different pH values by analytically pure H_2SO_4 (Tianjin Wind Boat Chemical Reagent Technology Co. Ltd., Tianjin, China). The material used for 3D printing is a photosensitive resin (codenamed YJ305, Ningbo JK Brothers 3D Material Technology Ltd., Ningbo, China), mainly composed of photosensitive prepolymer and photoinitiator.

The initial pH value of the aqueous solution was measured using a pH meter (PHSJ-4F, Shanghai INESA Scientific Instrument Co. Ltd., Shanghai, China). The concentration of In^{3+} and Fe^{3+}in the initial solution and the raffinate was measured by inductively coupled plasma spectrometer. The concentration of metal ions in organic phase was calculated according to the law of conservation of mass from each experiment. The extraction rate (E), the distribution ratio (D), and the separation coefficient $\left(\beta_{In^{3+}/Fe^{3+}}\right)$ were calculated by the correlation formula as follows:

$$E(\%) = \frac{C_{aq,in} - C_{aq,out}}{C_{aq,in}} \times 100\% \quad (1)$$

$$D = \frac{C_{org}}{C_{aq}} \quad (2)$$

$$\beta_{\frac{In^{3+}}{Fe^{3+}}} = \frac{D_{In^{3+}}}{D_{Fe^{3+}}} \quad (3)$$

where $C_{aq,in}$ and $C_{aq,out}$ are the concentrations of the metal ions of the solute in the inlet and outlet aqueous phases, respectively. C_{org} and C_{aq} are the concentrations of the extract in the organic phase and aqueous phase after extraction process, respectively.

The initial experimental conditions are as follows: the concentration of In^{3+} and Fe^{3+} in aqueous solution was approximately 3 g/l, initial pH value was in the range of 0.2–0.9. In addition, the extractant D2EHPA was mixed with 260# solvent oil to make the extractant D2EHPA occupy 30% of the volume ratio.

2.2 Apparatus and extraction procedure

The physical diagram of key parts of the 3D printer is shown in Figure 1A. When the printer starts functioning, the workbench drops down toward the bottom of the material box such that it is approximately 50 μm away from the bottom of material box, the liquid resin gets squeezed into a thin slice, and then the printer program controls the ultraviolet light source to irradiate the resin through the transparent part of the material box. Subsequently, the monolayer resin so formed becomes solidified and left on the workbench, and the workbench goes back to the initial position. The workbench again descends to a height of 100 μm from the base of the material box and forms another layer. This is how the process of printing the designed microreactor is carried out layer by layer periodically until the completion of the model. The resin is mainly composed of approximately 30% acrylates, approximately 50% monomer (HDDA and TPGDA) as diluent, along with a small amount of assistants such as pigment, photoinitiators, and others. Because of commercial confidentiality considerations, detailed material formulation cannot be described here. According to the technical specifications, it is characterized by a critical energy (E_c) of 6–13 mJ/cm² and a penetration depth (D_p) of

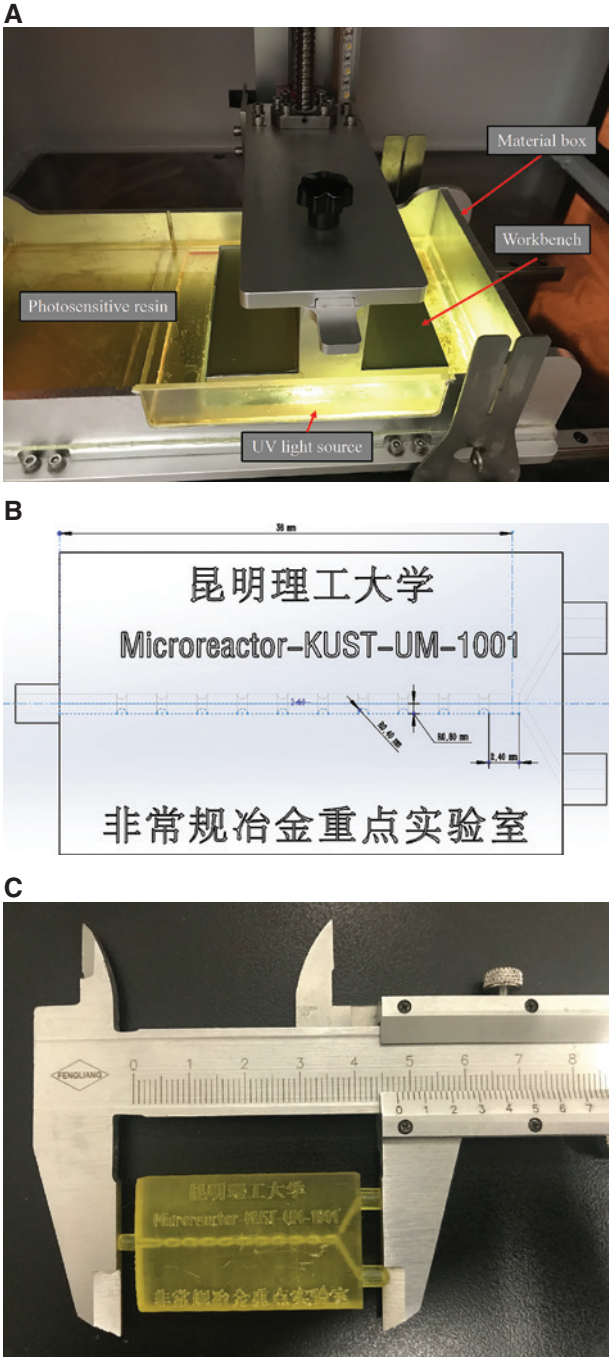

Figure 1: Physical diagram of the microreactor: (A) the physical diagram of key parts of the 3D printer, (B) 3D design diagram of the "Y"-shaped microreactor, (C) practical picture of the "Y"-shaped microreactor.

0.16–0.2 mm. The "Y"-shaped microreactor used in the experiment was made by using a quasi-industrial grade 3D printer (Mar2, Ningbo JK Brothers 3D Technology Co. Ltd.), and the resin was provided by Ningbo Yongju 3D Technology Co. Ltd.

The simple print operation process is as follows: 3D design→printing layout and slicing up→3D printing→postmolding treatment. The printing parameters were set as follows: single layer

thickness was 50 μm, single layer curing time was 8.5 s, and the wavelength of the UV LED was 405 nm.

Figure 1B and C show the design diagram of microchannel structure and the practical picture, respectively. The cross-sectional diameter of the mixing channel in the microreactor changes alternatively between 1600 and 800 μm, the total length of the mixing channel was 36 mm; as a result, the total volume of the mixing channel was approximately 0.0504 cm^3. The inner diameter of the inlet and outlet of the reactor was 1600 μm, which matches with the polytetrafluoroethylene (PTFE) capillary of the outer diameter (1600 μm) to ensure that liquid leakage will not occur during the experiment.

As the mixed fluids move from the wide passage to the narrow passage of the mixed channel, at a certain velocity, there will be a tendency to focus. Because the velocity of the fluid in the middle axis of the channel is greater than the velocity near the pipe wall position, a vortex will be formed inside the fluid, and the circulation speed will be accelerated in the narrow part of the channel. This phenomenon can strengthen the molecular diffusion process effectively at the interface of the two immiscible phases, thus a better extraction effect can be achieved [25]. The schematic diagram of flow pattern in the microchannel of the "Y"-shaped microreactor is shown in Figure 2.

Figure 3A shows the schematic diagram of the process of extraction and separation experiment. The organic phase and aqueous phase solution were injected using two 20-ml syringes (Jiangxi Qiao Ming Medical Instrument Co. Ltd.) simultaneously. Translucent PTFE capillary with 1.6 mm external diameter (Shanghai Wen Chang chip Co. Ltd.) was used to connect the entrances of the 3D-printed "Y" type microreactor to the organic phase syringe and the aqueous phase syringe. The organic phase and aqueous phase were pumped into the reactor with two digital injection pumps (RSPO1-B, Jiashan Rui Chong Electronic Technology Co. Ltd.). The flow velocity and contact time of the two immiscible liquids in the mixing channel of the microreactor were precisely controlled.

Figure 3B shows the experimental setup of the extraction process. The flow rate of both phase fluids was set by RSPO1-B digital injection pump, in which the contact time of the two immiscible phases in the mixing channel of the "Y"-shaped microreactor was controlled. The mixed liquid from the outlet of the reactor was collected by a separating funnel and the raffinate was collected in a test tube. The conventional extraction was carried out by separating funnel shacking method, as shown in Figure 3C. A total of 15 ml of the aqueous phase and 15 ml of the organic phase were poured into a separating funnel, placed in ZD-85 thermostat steam bath vibrator (Jintan Development Zone Jeater Experimental Instrument Factory) with 300 r/min frequency of oscillation for a certain period of time, then the raffinate was collected for analysis. The experimental results of conventional extraction were compared with the extraction in the "Y"-shaped microreactor.

Figure 3D shows the flow details of the "Y"-shaped microreactor in the extraction process. It is clear that the regular slug flow formed in the mixing channel and capillary of the outlet was different from the stable laminar flow observed by Li et al. [10] in their investigation on the extraction of In^{3+} in a double "Y" type microfluidic chip. The reason is that the width of the "Y" reactor used in the present study was approximately 10 times larger than that of the microfluidic chip in the study by Li et al. In addition, the cross-sectional area of the mixing channel was not fixed, which results in the alternate change of Reynolds number (*Re*) in the mixing channel. This effect can refresh the interface of the two immiscible phases frequently, so it is advantageous to improve the efficiency of extraction [26].

3 Results and discussion

3.1 Effect of initial aqueous phase pH value

According to Wang [1], with the decrease in the initial pH value of the aqueous phase, the ability of D2EHPA to extract Fe^{3+} will decrease sharply, especially under the pH value of 1.5 [1]. In contrast, the decrease of initial pH has very small influence on the extraction of In^{3+}. Therefore, the appropriate initial pH value is an important factor in the extraction and separation of In^{3+} and Fe^{3+} in the solution.

The volume flow of the two phases in this experiment was 7.2 μl/min, the contact time of the two immiscible liquids in the mixing channel of the "Y"-shaped microreactor was 210 s, and the phase ratio (O/A) was 1:1. The volume fraction of D2EHPA in the 260# solvent oil was 30%, the concentration of In^{3+} in the initial aqueous was in the range of 2.41–2.59 g/l, and the Fe^{3+} in the initial aqueous was in the range of 1.48–2.12 g/l.

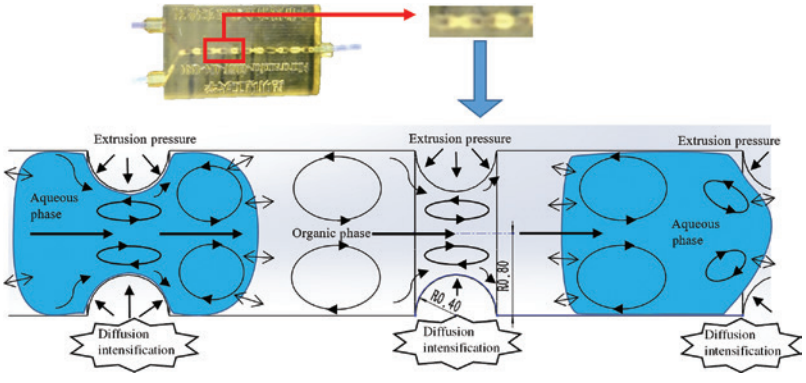

Figure 2: Schematic diagram of internal flow pattern in the microchannel of the "Y" microreactor.

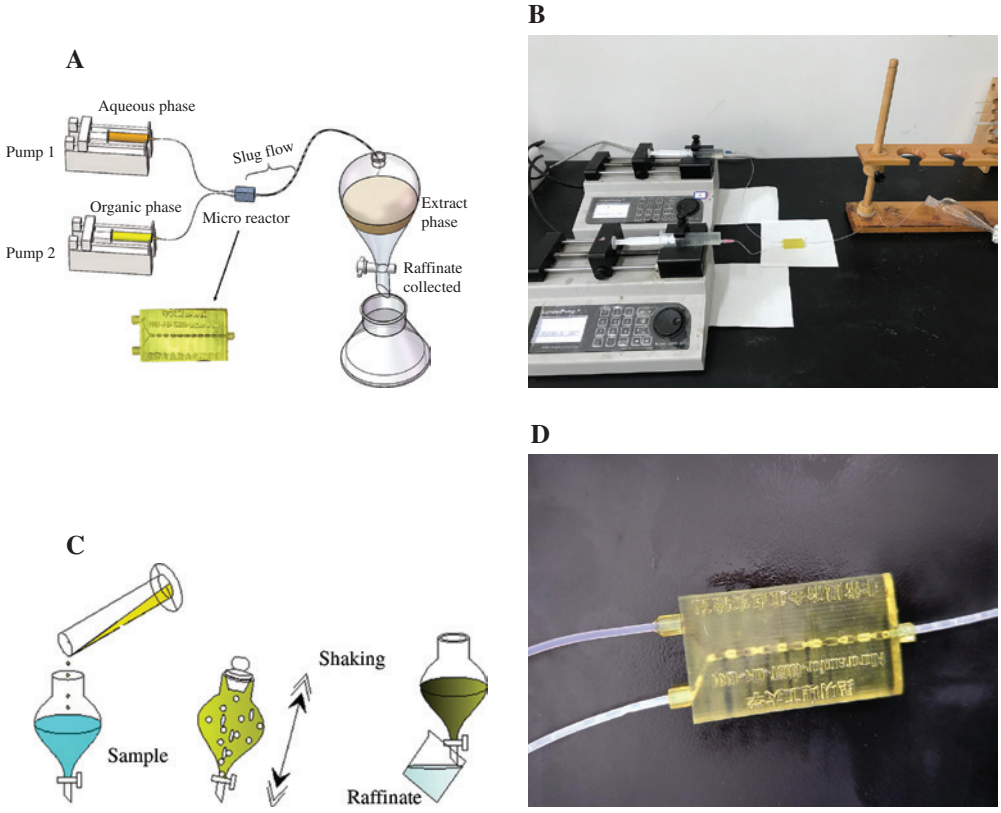

Figure 3: Flow diagram of extraction experiment: (A) schematic diagram of the process of extraction, (B) practical picture of the extraction experiment, (C) separating funnel shaking method to imitate conventional extraction in industrial devices, (D) flow details in the microreactor during extraction.

As shown in Figure 4A, extraction rate of In^{3+} increases gradually when the initial pH value of aqueous phase increased from 0.2 to 0.7 in microchannel, whereas the extraction rate of Fe^{3+} has been increased continuously in the oscillating extraction. Extraction rate of In^{3+} in "Y"-shaped microchannel reactor and the shaker are as high as 98.15% and 98.07%, respectively, whereas the extraction rate of Fe^{3+}under the oscillating condition (13.40%) is much higher than the extraction rate (3.09%) in the "Y"-shaped microreactor. The extraction rate of In^{3+} at pH value of 0.9 is close to that of at pH value of 0.7 in both the methods. According to Figure 4B, the separation coefficient $\beta_{In/Fe}$ in the "Y" type microchannel reactor is much higher than that of oscillating extraction, and the separation effect is optimal at the pH value of 0.7.

3.2 Effect of contact time

From the macroscopic view, there is a stable interface between the two immiscible phases. The metal ions in aqueous phase require a certain time to diffuse into the interface to form complexes with organic molecules and then become dissolved in the organic phase. The extraction rate of the metal ions increases by extending the contact time of the two immiscible liquids, which also increases the extraction rate of impurity ions (Fe^{3+} in this study) [27–29], so it is important to control the contact time of liquids to obtain a high separation coefficient $\beta_{In/Fe}$.

The initial pH value of the aqueous was adjusted to 0.5, the volume fraction of D2EHPA was 30% and the phase ratio (O/A) was 1:1. Each phase flow rate was controlled by the digital injection pump (RSPO1-B) to ensure the contact time of two immiscible phases in the microchannel was in the range of 3–210 s.

The experimental results are shown in Figure 5. The extraction rate of In^{3+} in the "Y"-shaped microreactor increases with the increase of contact time, and it changes significantly in the range of 3–150 s. However, the extraction rate of In^{3+} changes a little when the contact time is more than 150 s. When the contact time is 150 s, the extraction rate of In^{3+} reaches 89.51%, which is very close to the 90.12% observed at 210 s. At this point, the separation coefficient $\beta_{In/Fe}$ changes slightly and it begins to decrease

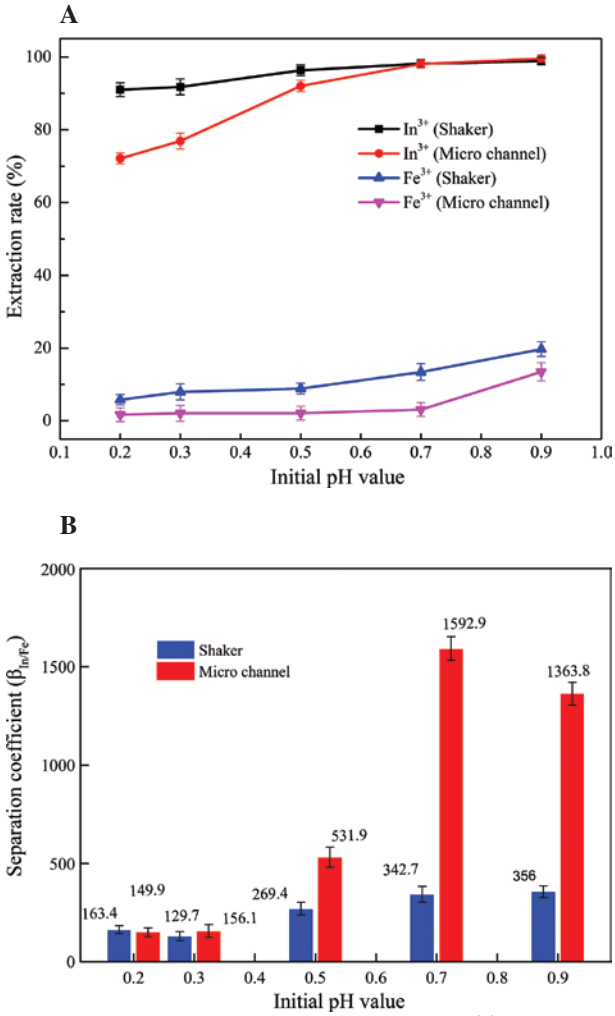

Figure 4: Effect of initial aqueous phase pH value: (A) effect of initial pH value on the extraction efficiency, (B) effect of initial pH value on the separation coefficient. Aqueous phase: $[In^{3+}] = 2.59$ g l^{-1}, pH = 0.2–0.9, $[Fe^{3+}] = 2.12$ g l^{-1}; organic phase: $\varphi_{D2EHPA} = 30\%$; O/A = 1:1, $Q = 7.2$ µl/min, $T = 298$ K.

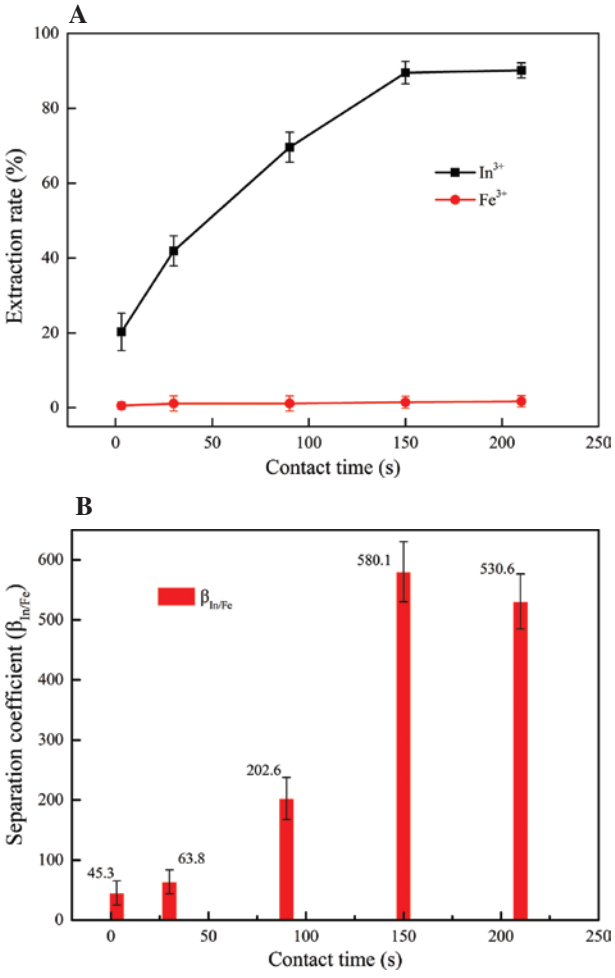

Figure 5: Effect of contact time: (A) effect of initial contact time on the extraction efficiency, (B) effect of contact time on the separation coefficient. Aqueous phase: $[In^{3+}] = 2.59$ g l^{-1}, pH = 0.5, $[Fe^{3+}] = 2.12$ g l^{-1}; organic phase: $\varphi_{D2EHPA} = 30\%$; O/A = 1:1, $Q = 7.2$–504 µl/min, $T = 298$ K.

from 580.1 to 530.6. Hence, it is inferred that the extraction of In^{3+} in the aqueous phase is almost approaching equilibrium in the mixing microchannel of the "Y"-shaped microreactor at a contact time of 150 s.

At the same time, the extraction rate of Fe^{3+} varies slightly with the contact time. It might be due to the relatively poor selective extraction ability of D2EHPA to Fe^{3+} at the pH value of 0.5. According to the observations in Subsection 3.1, the initial aqueous phase pH value is the main controlling factor for Fe^{3+} extraction. Whereas in this subsection, the experimental results demonstrate that the contact time (or the residence time) is the main controlling factor for In^{3+} extraction in the microchannel of the "Y"-shaped microreactor for the mixed liquid. Therefore, a relatively high separation coefficient $\beta_{In/Fe}$ can be obtained by controlling the contact time of two immiscible liquids to 150 s in the mixing microchannel.

3.3 Effect of phase ratio (O/A)

The principle of solvent extraction is to separate the mixture according to the different solubilities of the material in two immiscible solvents. The extractable ions will be encapsulated by the extractant molecules more easily if the amount of extractant increases. Therefore, the volume ratio of organic phase to aqueous phase has an effect on the results of extraction and separation of metal ions. In consideration of the extraction process in industrial production, excessive O/A might cause too much consumption of extractant, which will result in unnecessary waste/potential danger and make the stripping process more difficult. Hence, it is

necessary to investigate the effect of phase ratio (O/A) on extraction and separation efficiency in detail.

In this study, the initial aqueous pH value was adjusted to 0.5, the volume fraction of extract in 260# solvent oil was 30%, and the contact time of two immiscible phases in the mixing microchannel of the "Y"-shaped microreactor was 150 s. The same conditions were used in the conventional oscillating extraction in separating funnel by ZD-85 thermostatic oscillator with oscillation frequency is 300 rpm.

Figure 6A reveals that the extraction rate of In^{3+} decreases slightly from 99.9% to 96.4%, whereas the extraction rate of Fe^{3+} changes significantly from 31.5% to 11.1%, in the oscillating extraction method when O/A > 1. On the other hand, the extraction rate of In^{3+} varies from 98.5% to 91.0% and the extraction rate of Fe^{3+} varies from 12.3% to 1.93% in the "Y" microreactor. Compared with the oscillating extraction method, the extraction reaction of the mixed fluid occurred in relatively mild environment in the microreactor, which is different from the mixed, disordered, and oscillating environment. Mixed fluid forms a stable slug flow pattern in the mixing microchannel. Different phase ratio (O/A) results in a corresponding change in the proportion of oil phase and aqueous phase in mixing channel of the microreactor (including the capillary from the outlet of microreactor to the separating funnel) [30, 31], so the extraction rate curve of In^{3+} in the microchannel is close to a straight line.

Figure 6B shows the significant effect of phase ratio (O/A) on separation coefficient $\beta_{In/Fe}$. The separation coefficient $\beta_{In/Fe}$ of oscillating extraction declined rapidly with the decreasing of the phase ratio (O/A), and the separation efficiency of the microreactor extraction was better than that of the oscillating extraction when O/A ≤ 1, which is similar to the industrial production. It is therefore inferred that the high ratio of aqueous phase has better separation efficiency in the microreactor extraction method. If this can be applied to the industrial scale, it is very useful to avoid the problem of excessive amounts of extractant.

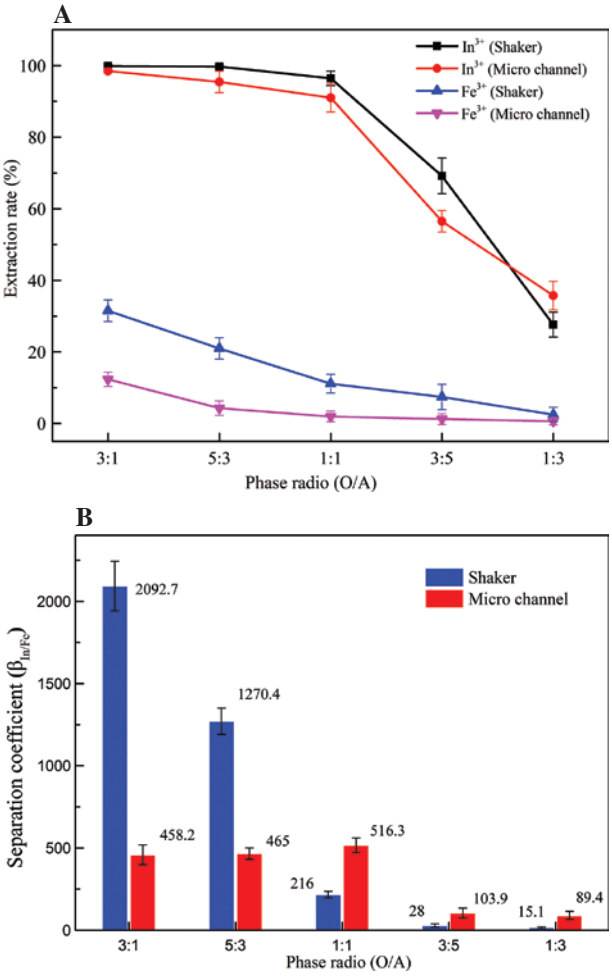

Figure 6: Effect of phase ratio (O/A): (A) effect of phase ratio (O/A) on the extraction rate, (B) effect of phase ratio (O/A) on the separation coefficient. Aqueous phase: $[In^{3+}] = 2.59$ g l^{-1}, pH = 0.5, $[Fe^{3+}] = 2.12$ g l^{-1}; organic phase: $\varphi_{D2EHPA} = 30\%$; O/A = 3:1–1:3, $Q = 20.16$ µl/min, $T = 298$ K.

3.4 Comparison with smaller size reactor

Li et al. [10] used some commercial microchips with microchannels (50 µm × 100 µm) to investigate the regularity of extraction of In^{3+}. D2EHPA was used as an extractant in the study, the extraction rate of In^{3+} reached 99.9% when the contact time was only approximately 1 s. If the size of channel in the chip is changed to 100 µm × 200 µm, it requires 7 s for the extraction rate of In^{3+} to reach 99% under the same conditions. The influence of microreactor characteristics on the extraction effect of In^{3+} is listed in Table 1, which proves that the effect of the size of the mixing channel on extraction rate is significant [10, 32].

However, the extremely low handling capacity is a difficult problem to apply these microfluidic chips in industrial extraction processes. Besides, the relatively high cost to produce polydimethylsiloxane (PDMS) microchips using existing processing technologies such as LIGA, etching, or precision machining is disadvantageous [12], and there exists no better method to reproduce, expand, or optimize the structure in an efficient way, limiting the related research development of microfluidic extraction.

To fabricate the "Y"-shaped microreactor in this work, 12 g of resin, whose market price is approximately 1170 yuan per kilogram, was consumed, the maximum power of the printer was 450 W, and the time taken was approximately 4 h, and so, coupled with the depreciation of the 3D printer,

Table 1: The influence of microchannel characteristics on In^{3+} extraction.

Microreactor	Shape of cross-section	Characteristic dimensions (μm)	Channel length (mm)	Extraction rate of In^{3+} (%)	Handling capacity (ml/min)
Double "Y" (PDMS)	Square	100×50	120	99.9	~0.02
Double "Y" (PDMS)	Square	200×100	120	99.9	~0.02
Double "Y" (PDMS)	Square	1000×50	120	87.1	0.5
"Y"-shaped (3D printed)[a]	Round	800–1600	36	98.1	0.072

[a]In this work.

the total manufacturing cost of the "Y"-shaped microreactor is estimated to be less than 20 yuan. The PDMS chips in Table 1 were provided by Suzhou Wen Hao Chip Technology Co. Ltd., the market price of which is more than 350 yuan each. Therefore, the 3D printing method for making microreactor in this work is better from an economic perspective.

The advantage of the "Y" microreactor used in this study is shown in Table 1, comparing with the other microreactors of smaller characteristic size. The 3D-printed "Y"-shaped microreactor could yield a high extraction rate of In^{3+} although the length of the mixed channel is shorter and its feature size is larger. This is due to the enhancement of diffusion at the interface of two immiscible phases by the focusing flow pattern in the mixing channel as mentioned in Subsection 2.2. In addition, with the help of 3D printing technology, it is easy to make a single channel duplicated into multichannel production, so that the amount of processing in the microreactor can be expanded by a great deal.

Emerging 3D printing technologies have produced a variety of reactors with complex constructions in a very short time with low cost and limited manual labor. It relies on its characteristics of digital, rapid prototyping, additive manufacturing, and so on. Theoretically, the design and optimization of the mixing channel of the "Y" type structure reactors mentioned in this article can be carried out, and its mixing channel can be replicated and expanded, which can greatly improve the throughput of microreactors [33]. For example, up to 150 microchannels can be achieved in the microreactor using 3D printing. Currently, our research group is focusing on related experiments at the Key Laboratory of Unconventional Metallurgy in Kunming University of Science and Technology.

4 Conclusions

According to the results of the separation of In^{3+} by "Y"-shaped microreactor and conventional separating funnel, it is preliminarily recognized that the 3D printing microreactor has broad prospects for solvent extraction and separation and the following main conclusions can be drawn:

1. The focused flow in microchannels can significantly enhance the diffusion efficiency of two immiscible phase fluids, and enable the microchannel to obtain a relatively high extraction rate under shorter length and larger characteristic size.
2. A "Y"-shaped microreactor with a channel size of 800–1600 μm was successfully developed by 3D printing technology and applied to extract and separate In^{3+} and Fe^{3+}. The two immiscible phases formed a stable slug flow in the mixing microchannel. When the pH value was in the range of 0.7–0.9, the extraction rate of In^{3+} in the "Y" microreactor was quite close to the oscillating extraction, more than 98%. However, the extraction rate of Fe^{3+} in oscillating extraction was much higher in the "Y" microreactor, resulting in better β_{Micro} coefficient than $\beta_{Oscillation}$ coefficient.
3. The extraction of In^{3+} with microreactor was close to the extraction equilibrium when the contact time was more than 150 s. Contact time was the main controlling factor for the extraction of In^{3+} and the pH value was the main controlling factor for the extraction of Fe^{3+}.
4. The separation efficiency of microreactor extraction was better than that of oscillating extraction when $O/A \leq 1$. The separation efficiency of microreactor increased gradually with the decrease of O/A and the separation coefficient $\beta_{In/Fe}$ reached the optimal value when the $O/A = 1$.

Acknowledgements: The authors acknowledge the financial support provided by the National Natural Science Foundation of China (no. 51104073), Applied Basic Research Program of Yunnan Province (2015FA017), and Yunnan Provincial Science and Technology Innovation Talents Scheme – Technological Leading Talent (2013HA002). Sivasankar Koppala especially thanks Kunming University of Science and Technology for a post-doctoral fellowship.

References

[1] Wang, S. *Indium Metallurgy*, Metallurgical Industry Press: Beijing, 2006.
[2] Li X, Wei C, Deng Z, Li C, Fan G, Rong H, Zhang F. *Sep. Purif. Technol.* 2015, 156, 348–355.
[3] Guo T, Li C, Liu D. *Non-ferrous Mining and Metallurgy* 2000, 6, 18–22.
[4] Kralj JG, Sahoo HR, Jensen KF. *Lab Chip* 2007, 7, 256–263.
[5] Ciceri D, Perera JM, Stevens GW. *J. Chem. Technol. Biotechnol.* 2014, 89, 771–786.
[6] Kenig EY, Su Y, Lautenschleger A, Chasanis P, Grünewald M. *Sep. Purif. Technol.* 2013, 120, 245–264.
[7] Maruyama T, Kaji T, Ohkawa T, Ohkawa T, Sotowa KI, Matsushita H, Kubota F, Kamiya N, Kusakabe K, Goto M. *Analyst* 2004, 129, 1008–1013.
[8] Novak U, Pohar A, Plazl I, Žnidaršič-Plazl P. *Sep. Purif. Technol.* 2012, 97, 172–178.
[9] Rahimi M, Aghel B, Hatamifar B, Akbari M, Alsairafi AA. *Chem. Eng. Process.* 2014, 86, 36–46.
[10] Li C, Jiang F, Ju S, Peng J, Wei Y, Zhang L. *Can. Metall. Q.* 2016, 54, 432–438.
[11] Darekar M, Singh KK, Mukhopadhyay S, Shenoy KT. *Sep. Purif. Technol.* 2016, 158, 160–170.
[12] Ehrfeld W, Hessel V, Löwe H. *Microreactors: New Technology for Modern Chemistry*, Wiley-VCH Verlag GmbH & Co. KGaA: Hoboken, 2000.
[13] McCreedy T. *TrAC, Trends Analyt. Chem.* 2000, 19, 396–401.
[14] Gibson I, Rosen D, Stucker B. *Assembly Automation* 2015, 32.
[15] O'Connor J, Punch J, Jeffers N, Stafford J. *J. Phys. Conf. Ser.* 2014, 525, 1055–1061.
[16] Wu H, Brittain S, Anderson J, Grzybowski B, Whitesides S, Whitesides GM. *J. Am. Chem. Soc.* 2000, 122, 12691–12699.
[17] Kashid MN, Gupta A, Renken A, Kiwi-Minsker L. *Chem. Eng. J.* 2010, 158, 233–240.
[18] Saber M, Commenge JM, Falk L. *Chem. Eng. Sci.* 2010, 65, 372–379.
[19] Credi C, Pintossi D, Bianchi CL, Levi M, Griffini G, Turri S. *Mater. Des.* 2017, 133, 143–153.
[20] Griffini G, Invernizzi M, Levi M, Natale G, Postiglione G, Turri S. *Polymer* 2016, 91, 174–179.
[21] Invernizzi M, Natale G, Levi M, Turri S, Griffini G. *Materials* 2016, 9, 583.
[22] Chen K, Kuang X, Li V, Kang G, Qi HJ. *Soft Matter* 2018, 14, 1879.
[23] Credi C, Griffini G, Levi M, Turri S. *Small* 2018, 14, 1702831.
[24] Iwasaki T, Kawano N, Yoshida J. *Org. Process Res. Dev.* 2006, 10, 1126–1131.
[25] Anna SL, Bontoux N, Stone HA. *Appl. Phys. Lett.* 2003, 82, 364–366.
[26] Mark D, Haeberle S, Roth G, Von SF, Zengerle R. *Chem. Soc. Rev.* 2010, 39, 1153.
[27] Yin S, Zhang L, Peng J, Li S, Ju S, Zhang L. *Chem. Eng. Process.* 2015, 91, 1–6.
[28] Zhang L, Hessel V, Peng J, Wang Q, Zhang L. *Chem. Eng. J.* 2017, 307, 1–8.
[29] Yang L, Zhao Y, Su Y, Chen G. *Chem. Eng. Technol.* 2013, 36, 985–992.
[30] Tamagawa O, Muto A. *Chem. Eng. J.* 2011, 167, 700–704.
[31] Ufer A, Mendorf M, Ghaini A, Agar DW. *Chem. Eng. Technol.* 2015, 34, 353–360.
[32] Ueno K, Kim HB, Kitamura N. *Anal. Sci.* 2003, 19, 391.
[33] Greenway GM, Haswell SJ, Morgan DO, Skelton V, Styring P. *Sens. Actuators B* 2000, 63, 153–158.